



Integrating Network Analysis and Metabolomics to Reveal Mechanism of Huaganjian Decoction in Treatment of Cholestatic Hepatic Injury

Qin Dong¹, Jiao Chen¹, Yan-Ping Jiang¹, Zong-Ping Zhu¹, Yong-Feng Zheng¹, Jin-Ming Zhang¹, Zhen Zhang¹, Wen-Qing Chen², Shi-Yi Sun¹, Lan Pang¹, Xin Yan³, Wan Liao^{1*} and Chao-Mei Fu^{1*}

¹State Key Laboratory of Southwestern Chinese Medicine Resources, Pharmacy College, Chengdu University of Traditional Chinese Medicine, Chengdu, China, ²Department of Biology, Hong Kong Baptist University, Hong Kong, China, ³Chengdu Institute of Chinese Herbal Medicine, Chengdu, China

OPEN ACCESS

Edited by:

Zhong-qiu Liu,
Guangzhou University of Chinese
Medicine, China

Reviewed by:

Elisa Lozano,
University of Salamanca, Spain
Gang Cao,
Zhejiang Chinese Medical University,
China

*Correspondence:

Wan Liao
liaowan@cdutcm.edu.cn
Chao-Mei Fu
chaomeifu@126.com

Specialty section:

This article was submitted to
Ethnopharmacology,
a section of the journal
Frontiers in Pharmacology

Received: 10 September 2021

Accepted: 22 December 2021

Published: 19 January 2022

Citation:

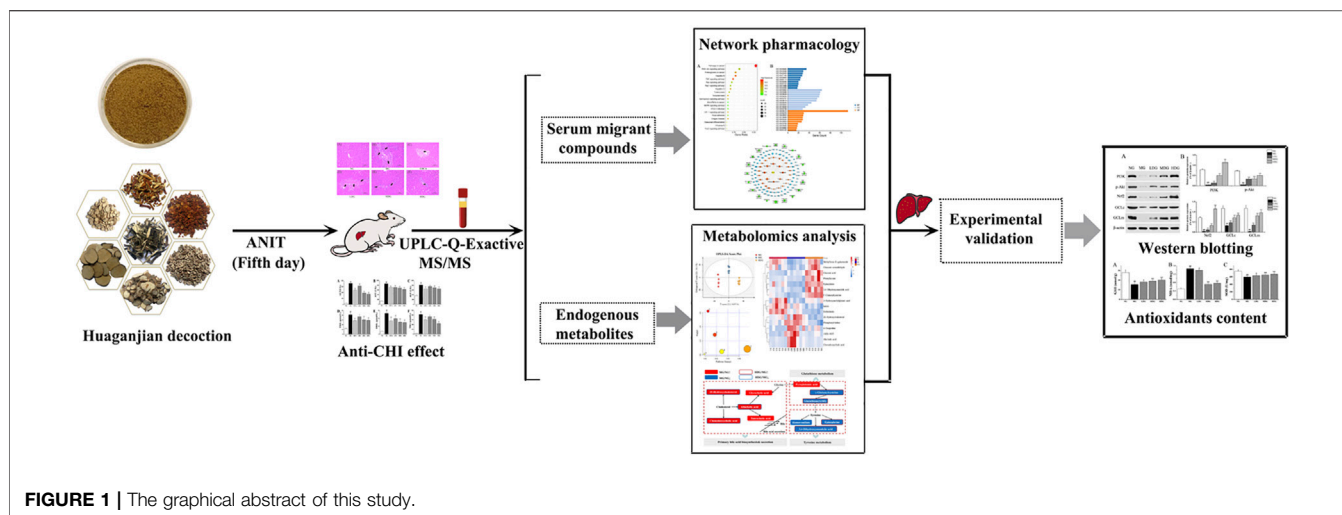
Dong Q, Chen J, Jiang Y-P, Zhu Z-P,
Zheng Y-F, Zhang J-M, Zhang Z,
Chen W-Q, Sun S-Y, Pang L, Yan X,
Liao W and Fu C-M (2022) Integrating
Network Analysis and Metabolomics to
Reveal Mechanism of Huaganjian
Decoction in Treatment of Cholestatic
Hepatic Injury.
Front. Pharmacol. 12:773957.
doi: 10.3389/fphar.2021.773957

Huaganjian decoction (HGJD) was first recorded in the classic “*Jing Yue Quan Shu*” during the Ming dynasty, and it has been extensively applied in clinical practice to treat liver diseases for over 300 years in China. However, its bioactive constituents and relevant pharmacological mechanism are still unclear. In this study, a strategy integrating network analysis and metabolomics was applied to reveal mechanism of HGJD in treating cholestatic hepatic injury (CHI). Firstly, we observed the therapeutic effect of HGJD against CHI with an alpha-naphthylisothiocyanate (ANIT) induced CHI rat model. Then, we utilized UPLC-Q-Exactive MS/MS method to analyze the serum migrant compounds of HGJD in CHI rats. Based on these compounds, network analysis was conducted to screen for potential active components, and key signaling pathways interrelated to therapeutic effect of HGJD. Meanwhile, serum metabolomics was utilized to investigate the underlying metabolic mechanism of HGJD against CHI. Finally, the predicted key pathway was verified by western blot and biochemical analysis using rat liver tissue from *in vivo* efficacy experiment. Our results showed that HGJD significantly alleviated ANIT induced CHI. Totally, 31 compounds originated from HGJD have been identified in the serum sample. PI3K/Akt/Nrf2 signaling pathway related to GSH synthesis was demonstrated as one of the major pathways interrelated to therapeutic effect of HGJD against CHI. This research supplied a helpful strategy to determine the potential bioactive compounds and mechanism of traditional Chinese medicine.

Keywords: huaganjian decoction, cholestatic hepatic injury, metabolomics, serum pharmacology, network analysis

1 INTRODUCTION

Cholestatic hepatic injury (CHI) occurs mainly due to intrahepatic cholestasis. Its main characteristics are aberrant metabolism of bile acid and accumulating of toxic bile acids in the liver. Signals such as oxidative stress and inflammatory responses are activated, leading to parenchymal cell death of liver and bile duct (Cai and Boyer, 2021). Without proper treatment, CHI may further develop into fibrosis, cirrhosis, hepatocellular carcinoma and eventually liver failure



(Pollock and Minuk, 2017). Currently, ursodeoxycholic acid (UDCA), and obeticholic acid (OCA) are main therapeutic options for CHI (Hohenester and Beuers, 2017). However, some patients have an inadequate response to UDCA therapy and the side effects of OCA in this treatment remain to be improved (Hirschfield et al., 2015; Kowdley et al., 2018).

In recent years, with rapid preclinical and clinical research of traditional Chinese medicine (TCM), TCM has shown advantage in clinical practice to treat CHI. Huaganjian decoction (HGJD) is a classic Chinese medicine formula, which is first recorded in the classic “*Jing Yue Quan Shu*” during the Ming dynasty. This formula is composed of 7 botanical drugs: Citri Reticulatae Pericarpium Viride (*Citrus reticulata* Blanco, Qingpi, 7.5 g), Gardeniae Fructus (*Gardenia jasminoides* Ellis, Zhizi, 5.6 g), Paeoniae Radix Alba (*Paeonia lactiflora* Pall., Baishao, 7.5 g), Moutan Cortex (*Paeonia suffruticosa* Andr., Mudanpi, 5.6 g), Alismatis Rhizaoma (*Alisma plantago-aquatica* Linn., Zexie, 5.6 g), Fritillariae Thunbergii Bulbus (*Fritillaria thunbergii* Miq., Zhebeimu, 11.2 g), and Citri Reticulatae Pericarpium (*Citrus reticulata* Blanco, Chenpi, 7.5 g). It is characterized by comprehensive therapy, which can relieve stagnation of liver qi, extenuate liver fire, and invigorate liver blood. It was widely used in the clinical practice to protect against liver injury (He, 2009; Liu L F et al., 2019; Li, 2021). Moreover, HGJD has been listed as one of the 100 ancient classic prescriptions highly valued by the Chinese government. According to modern medical research, HGJD could promote bile excretion, protect liver cells, and inhibit the proliferation of activated hepatic stellate cells HSC-T6 (Gao et al., 2019). Qingpi was the principle drug of HGJD, which could protect against liver damage caused by carbon tetrachloride and promote bile excretion (Jin et al., 2007). Zhizi was the minister drug of HGJD, which could attenuate live cell injury and fibrosis as demonstrated in both animal and human studies (Chen et al., 2012). However, the specific mechanism of HGJD protecting against CHI is still not revealed. Besides, the bioactive compounds that contribute to its therapeutic efficacy remain unclear.

In this research, a comprehensive method integrating network analysis and metabolomics was used to illustrate mechanism of HGJD in treating CHI. Firstly, we observed the therapeutic effect of HGJD against CHI by evaluating the serum biochemical indices and histopathology of liver with an ANIT induced CHI rat model. Then, we utilized UPLC-Q-Exactive MS/MS method to analyze the serum migrant compounds of HGJD in ANIT induced CHI rat model. Network analysis based on serum migrant compounds of HGJD was used to explore the correlations among potential active ingredients, targets and signaling pathways interrelated to therapeutic effect of HGJD. Meanwhile, non-target serum metabolomics were applied to investigate the underlying metabolic mechanism of HGJD against CHI. Finally, we further validated the predicted pathway by western blot and biochemical analysis using rat liver tissue from *in vivo* efficacy experiment. This research would offer experimental basis for further research on HGJD in treatment of CHI, and offer a novel insight into improving the treatment for CHI. A graphical abstract of this study is presented in **Figure 1**.

2 MATERIALS AND METHODS

2.1 Chemicals and Reagents

All 22 standard compounds used in this study (synephrine, gallic acid, chlorogenic acid, geniposide, peimine, peiminine, albiflorin, paeoniflorin, rutin, narirutin, crocin, naringin, hesperidin, neohesperidin, didymin, quercetin, benzoylpaeoniflorin, paeonol, sinensetin, nobiletin, hepta-3, and alisol B 23-acetate) were supplied by Weikeqi Biotechnology Co., Ltd (Chengdu, China), and the purity were all greater than 98%. UDCA administrated as positive control was supplied by Shanghai Aladdin Biochemical Co., Ltd. (Shanghai, China). ANIT and medical-grade soybean oil were purchased from Shanghai Aladdin Biochemical Co., Ltd. (Shanghai, China). β -actin was obtained from Wuhan Servicebio Technology Co., Ltd. (Wuhan, China). Antibody PI3K was purchased from Beijing Boasosen

Biotechnology Co., Ltd. (Beijing, China). Antibody p-AKT was bought from Affinity Biosciences Ltd. (Jiangsu, China). Antibody Nrf2 was purchased from Wuhan Sanying Biotechnology Co., Ltd. (Wuhan, China). Antibody GCLc and GCLm were obtained from abcam (Cambridge, United Kingdom). Commercially available kits were provided by Nanjing Jian cheng Institute of Biotechnology (Nanjing, China) and Changchun Huili Biological Technology Co., Ltd. (Changchun, China). All other chemicals and reagents were belonged to analytical grade, and were purchased from commercial sources.

All botanical drugs in the HGJD formula were bought from Sichuan Neautus TCM Co., Ltd (Chengdu, China) and identified by Professor Guihua Jiang of the School of Pharmacy, Chengdu University of Traditional Chinese Medicine.

2.2 Preparation of HGJD Samples

The botanical drug mixture of Citri Reticulatae Pericarpium Viride, Gardeniae Fructus, Paeoniae Radix Alba, Moutan Cortex, Alismatis Rhizaoma, Fritillariae Thunbergii Bulbus, and Citri Reticulatae Pericarpium (4: 3: 4: 3: 3: 6: 4) was soaked with 9 vol. distilled water for 30 min and maintained boiling for 25 min. The extraction solution was filtered and evaporated under reduced pressure to the weight of the original mixture. Finally, freeze drying was carried out for concentrated extract to obtain lyophilized powder. The lyophilized powder yield was about 33.12%. The lyophilized powder was stored in different airtight packages before chemical and pharmacological studies. Quality control of the sample was led according to our previous research (Nie et al., 2020). Moreover, UPLC-Q-Exactive MS/MS was used to analyze the chemical composition of HGJD sample (**Supplementary Figure S1; Supplementary Table S1**). Every day before administration, lyophilized powder of HGJD was dissolved in different volumes of water to prepare low (0.15 g/ml), medium (0.30 g/ml) and high dosage (0.60 g/ml) samples.

2.3 Animals

SPF Male Sprague-Dawley (SD) rats (220 ± 20 g) were purchased from Beijing Sibefu Biotechnology Co., Ltd. (Beijing, China) (Certificate No. SCXK (Jing) 2019-0010). Animal Ethics Committee of Chengdu University of TCM (Chengdu, China) approved this experiment, and international rules for care and use of laboratory animals were strictly followed. The room temperature was regulated at 20 ± 2 °C with 50 ± 20% humidity and equipped with a 12 h light/dark cycle. We allowed the rats to eat pure water and food freely. All animals were adapted to the conditions for 1 week.

2.4 Anti-CHI Effect of HGJD

2.4.1 Animal Treatment

Thirty-six rats were randomly divided into six groups on average. Normal group (NG) and model group (MG) were received gavage of saline once daily for seven consecutive days. UDCA treated positive group (UDCA, 100 mg/kg), and three HGJD groups treated with low (LDG, 1.50 g/kg, extracts), medium (MDG, 3.01 g/kg, extracts), and high dosages (HDG, 6.02 g/kg, extracts) were received oral administration once daily for

seven consecutive days. The adult dosage of HGJD is 50.50 g (crude drug) daily. Based on the body surface area index and lyophilized powder yield (33.12%) (Nair et al., 2018), the animal dosage of HGJD is calculated, and low animal dosage equals to the clinical dosage. On the fifth day, normal group was received the vehicle (soybean oil) treatment by gavage, and the other groups were received 60 mg/kg ANIT dissolved in an equal volume of soybean oil by gavage. According to previous studies, this dose was known to induce cholestasis.

The rats were maintained fasting for 12 h before receiving the last dose of HGJD. 1 h after the last dose, rats were anesthetized with pentobarbital. Blood samples were collected from abdominal aorta. After that, the rats were sacrificed. Liver samples were dissected, and rinsed once with ice-cold normal saline. One part of each liver sample was stored at -80°C for western blot and biochemical index analysis, and the remaining specimens were set in 10% PBS-buffered formalin for histopathological analysis.

2.4.2 Assays of the Serum Enzymes and Components

The contents of alanine transaminase (ALT), aspartate transaminase (AST), alkaline phosphatase (ALP), γ -glutamyltranspeptidase (γ -GT), total bilirubin (TBIL), direct bilirubin (DBIL), and total bile acid (TBA) in serum were determined by commercial test kits.

2.4.3 Histological Examination

The liver tissue fixed with 10% PBS-buffered formalin, were embedded in paraffin, serially sectioned (5 μ m), and stained with nuclear dye (hematoxylin) and counterstain (eosin) for histological examination. Optical microscopy was applied to examine the histological section.

2.5 Identification of Serum Migrant Compounds of HGJD

2.5.1 Animal Treatment

Six rats received oral administration of HGJD (6.02 g/kg) for 7 consecutive days. At fifth day, ANIT was orally administered to rats in both the model group and the dose group. On the seventh day, after the orally administration of HGJD at 15 min, 30 min, 1, 2, 4, and 6 h, blood samples were taken from the angular vein of each rat. The serum samples collected from each rat at the different time points were mixed before sample processing.

2.5.2 Preparation of Samples

10 ml of 50% methanol was applied to dissolve HGJD powder (0.1 g), and then the samples were extracted for 30 min by ultrasonic extraction. The mixture was centrifuged at 13,000 rpm maintained for 15 min. Filter membrane (0.22 μ m) was used to filter the supernatant to obtain an injection sample.

1 ml serum sample was added with 3 ml methanol, then vortexed for 30 s and centrifuged at 13,000 rpm 4°C for 15 min to precipitate the protein. The supernatant was collected and dried with a nitrogen blowing concentrator. The residue was dissolved with 500 μ l of 50% methanol, and repeated the centrifugation procedure. Then, a filter membrane (0.22 μ m) was used to filter the supernatant to obtain an injection sample.

2.5.3 UPLC-Q-Exactive MS/MS Analysis

The Vanquish UHPLC system (Thermo Fisher Scientific, United States) equipped with Q Exactive quadrupole-electrostatic field orbitrap high-resolution mass spectrometer was applied to analyze HGJD powder and serum samples. Samples were separated on an ACQUITY UPLC®BEH C₁₈ column (2.1 × 100 mm 1.7 μm, Waters, United States). The mobile phase consisted of deionized water with 0.1% formic acid (A) and acetonitrile (B). The gradient elution procedure was as follows: 0–35 min, 5–95% B; 35–40 min, 95% B. The column temperature was maintained at 30°C. The flow rate was set at 0.4 ml/min.

All samples were analyzed in positive and negative ion modes, respectively. Mass spectrometry parameters were set as follows: nitrogen was selected as auxiliary gas and sheath gas. Flow rate was 10 L/min in positive mode and 35 L/min in negative mode. The voltage of the ion spray was 3 kV and –2.5 kV separately. The ion source temperature was kept at 320°C. Auxiliary gas heating temperature was maintained at 350°C. The fragment voltage was 50 V. Scan mass ratio was within the mass range of m/z 50–1000.

Compound Discoverer software (Thermo Fisher Scientific) was applied to analyze the LC-MS data. Components were identified by comparison of chemical information of reference substances, and initially identified with online databases (MZ cloud, MZ vault) and literatures.

2.6 Network Analysis

2.6.1 Target Prediction of the Active Ingredients of HGJD Against CHI

The serum migrant components which were regarded as potential effective ingredients were applied to identify potential treatment targets of HGJD against CHI. Meanwhile, several online databases have contributed to the research of possible therapeutic targets. We first searched the CAS and 3D molecular structures of the serum migrant components on PubChem. Secondly, the CAS or 3D molecular structures were imported into TCMSP (<http://tcmsp-e.com>), Swiss Target Prediction (<http://www.swisstargetprediction.ch/>), and PharmMapper Server (Version 2017) (<http://www.lilab-ecust.cn/pharmmapper/index.html>) (Wang et al., 2017) to explore potential targets of the compounds. Then, “cholestasis”, “cholestatic hepatic injury” and “cholestatic liver injury” were used as keywords in the online database, including GeneCards (<http://www.genecards.org/>), Disgenet (<https://www.disgenet.org/>), OMIM (<https://omim.org/>), and TTD (Wang et al., 2020) (<http://bidd.nus.edu.sg/group/ttd/>) to screen for disease targets. Besides, standardization of all targets was conducted on the Uniprot database (<https://www.uniprot.org/>). Finally, intersection targets of CHI and HGJD were picked out by an online Venn analysis tool (<http://bioinformatics.psb.ugent.be/webtools/Venn/>).

2.6.2 KEGG Pathways Analysis and GO Biological Process Enrichment

To clarify the function of the targets and their functions in signaling transduction, the DAVID 6.8 database was applied to evaluate the KEGG pathways and GO enrichment of the targets of HGJD against CHI.

2.6.3 Network Construction

Three visualized networks were visualized by Cytoscape 3.7.1: 1) Drug-components-targets network was the interaction network among HGJD, potential active components of HGJD, and intersection targets; 2) Protein-Protein Interaction (PPI) network showed the importance of the targets of the potential active compounds of HGJD associated with CHI; 3) Components-Targets-Pathways network provided a systematic understanding of the complex network among drug, components, targets, pathways, and disease.

2.7 Metabolomics Analysis

2.7.1 Sample Preparation

100 μl of thawed serum sample and 300 μl of methanol (precooled at –20°C) were added into 1.5 ml centrifuge tubes, and vortexed for 60 s, then solution was allowed to stand for 30 min at 4°C. Samples were centrifuged for 15 min at 12,000 rpm and 4°C to obtain supernatant. Each supernatant was added with internal standard (2-chlorophenoalanine 1 mg/ml), oscillated, mixed and filtered through 0.22 μm membrane to get the prepared sample for UPLC-MS analysis. Ultimately, 20 μl of each prepared sample was taken and mixed to obtain the QC sample (Dunn et al., 2011).

2.7.2 Chromatography and Mass Spectrometry Conditions

Chromatographic separation was completed on Thermo Ultimate 3000 system which was equipped with a Hyper gold C₁₈ (100 × 2.1 mm, 1.9 μm, and Thermo) column. Gradient elution of analyses was conducted with 0.1% formic acid in 5% acetonitrile(C) and 0.1% formic acid in acetonitrile (D) for positive ion mode. While, 0.05% acetic acid in 5% acetonitrile (A) and 0.05% acetic acid in acetonitrile (B) for negative mode. An incremental linear gradient of solvent B or D (v/v) was used as follows: 0–1.5 min, 0–20% B/D; 1.5–9.5 min, 20–100% B/D; 9.5–14.5 min, 100% B/D; 14.5–14.6 min, 100–5% B/D; 14.6–18 min, 5% B/D. The column flow rate and temperature were respectively set at 0.3 ml/min and 45°C. 3 μl of each sample was injected into UPLC-Q-Exactive MS/MS for analysis.

The experiments of ESI-MSⁿ were conducted on the Thermo Q Exactive mass spectrometer in positive and negative ion modes, respectively. Mass spectrometry parameters were set as follows: spray voltage was 3.0 kV in positive mode and –3.2 kV in negative mode. Sheath gas was kept at 45 arbitrary units, while auxiliary gas was 15 arbitrary units. The capillary temperature was maintained at 350°C. Full mass scan (m/z 70–1050) and HCD MS/MS spectra were recorded at a resolution of 70,000.

2.7.3 Data Processing and Analysis

Raw data acquired by Proteowizard software (v3.0.8789) was transformed into mzXML format (Smith et al., 2006). Peaks recognition, filtration and comparison were executed by R (v3.3.2) XCMS package. Besides, peak intensity has been normalized, so as to facilitate comparison of different magnitudes of data. Then, Principal Component Analysis (PCA), Partial Least Squares Discriminant Analysis (PLS-DA), and Orthogonal-Partial Least Squares-Discriminant Analysis (OPLS-DA) methods were conducted by software SIMCA-P (v13.0) and R language ropes package to analyze data in different groups.

Components with marked changes in the groups ($p < 0.05$ and VIP > 1) were chosen as differential biomarkers, which were tentatively identified with the exact molecular weight (error < 20 ppm). Moreover, the MS/MS fragmentation patterns of compounds were matched by METLIN database (<http://www.metlin.scripps.edu/>) and MoNA database (<https://mona.fiehnlab.ucdavis.edu/>).

To reveal the changing trends of the potential biomarkers and the callback effect of HGJD, the heatmap analysis was carried out by MetaboAnalyst 5.0 (<https://www.metaboanalyst.ca/MetaboAnalyst/>) and R version 3.0.3. The pathways analysis of differential metabolites was conducted with MetaboAnalyst 5.0.

2.8 Regulation of PI3K/Akt/Nrf2 Pathway

2.8.1 Western Blotting Assay

Samples have been processed and determined the concentrations of total protein with BCA kit, before western blotting assay to test the level of PI3K, p-Akt, GCLc, GCLm, and Nrf2. As for Nrf2, the nuclear and cytoplasmic extractions were carefully performed by extraction kits. Then, these extractions were detected by Western blot analysis for the presence of Nrf2. The samples with equal amount of total protein (100 μ g) were electrophoresed on a twelve alkyl sulfate polyacrylamide gel system consisted of 5% stacking gel and 8–15% resolving gel. The electrophoresed products were transferred onto polyvinylidene fluoride membrane. The membranes were blocked in 5% skimmed milk powder for 0.5 h at room temperature, subsequently incubated with specific primary antibodies overnight, including PI3K (1:1000), p-Akt (1:1000), Nrf2 (1:1000), GCLc (1:1000), GCLm (1:1000), and β -actin (1:3000). Next, washed and incubated with appropriate secondary antibody for 30 min. Ultimately, membranes were developed with chemiluminescent detection reagents and visualized with film. The relative expressions of PI3K, p-Akt, Nrf2, GCLc, and GCLm were quantified through optical density value utilizing an image processing system.

2.8.2 Biochemical Analysis of Antioxidant Compounds in Liver Tissue

Equal amount of Liver tissue (0.4 g) was carefully homogenized on ice with normal saline using a high speed tissue grinder to get a 1:10 (w/v) solution. Then the supernatants were tested using the GSH, MDA, and SOD assay kit according to the manufacturer's instructions.

3 RESULTS

3.1 Anti-CHI Effect Evaluation

The levels of ALT, AST, ALP, TBIL, DBIL, TBA, and γ -GT in the model group were significantly higher than that in the normal group ($p < 0.01$), indicating that ANIT successfully induced the CHI in rats. The levels of all factors in HGJD treatment groups were dose dependently lower than those in model group (Figure 2). In addition, the high dose and medium dose of HGJD groups showed similar preventive effect with UDCA group on CHI ($p < 0.01$), while low dose showed weaker. As shown in Figure 3, liver tissue of normal group displayed normal structure, while the specimens in the ANIT group observed spotty necrosis of liver cells. Administrating with 3.01 and 6.02 g/kg HGJD significantly reduced the trauma of liver tissue. The results showed that HGJD had a protective effect against ANIT-induced CHI.

3.2 Identification of Serum Migrant Compounds of HGJD

We established a UPLC-Q-Exactive MS/MS analysis method to analyze HGJD extracts and serum samples from rats after treatment of HGJD. The typical base peak chromatographs were shown in Supplementary Figure S1. On the basis of standards and related literatures, 31 compounds from HGJD in total were identified initially (Table 1). These compounds involved flavonoids, organic acids, phenols, alkaloids, and terpenoids. According to previous research, above compounds might originate from Citri Reticulatae Pericarpium Viride, Gardeniae Fructus, Paeoniae Radix Alba, Moutan Cortex, Alismatis Rhizaoma, Fritillariae Thunbergii Bulbus, and Citri Reticulatae Pericarpium in HGJD. Detailed source for each compound was shown in Table 1. In this study, prototype compounds absorbed into serum were mainly focused on. However, the metabolites in serum have not been identified and classified.

3.3 Network Analysis

3.3.1 Targets Prediction of Potential Active Compounds of HGJD Against CHI

On the basis of 31 serum migrant compounds of HGJD, 596 targets of HGJD were picked. According to database analysis of disease targets, we obtained 962 targets. Subsequently, an online Venn analysis tool was applied to generate the Venn diagram. 159 common targets were regarded as potential targets of HGJD against CHI (Supplementary Figure S2, Table S2).

3.3.2 KEGG Pathways Analysis and Gene Ontology (GO) Enrichment

The enrichment of signaling pathways was performed on DAVID database, and top 20 KEGG pathways which were selected according to the order of p value from small to large, were shown in Figure 4A; Supplementary Table S3. The results demonstrated that HGJD treating CHI mainly involved

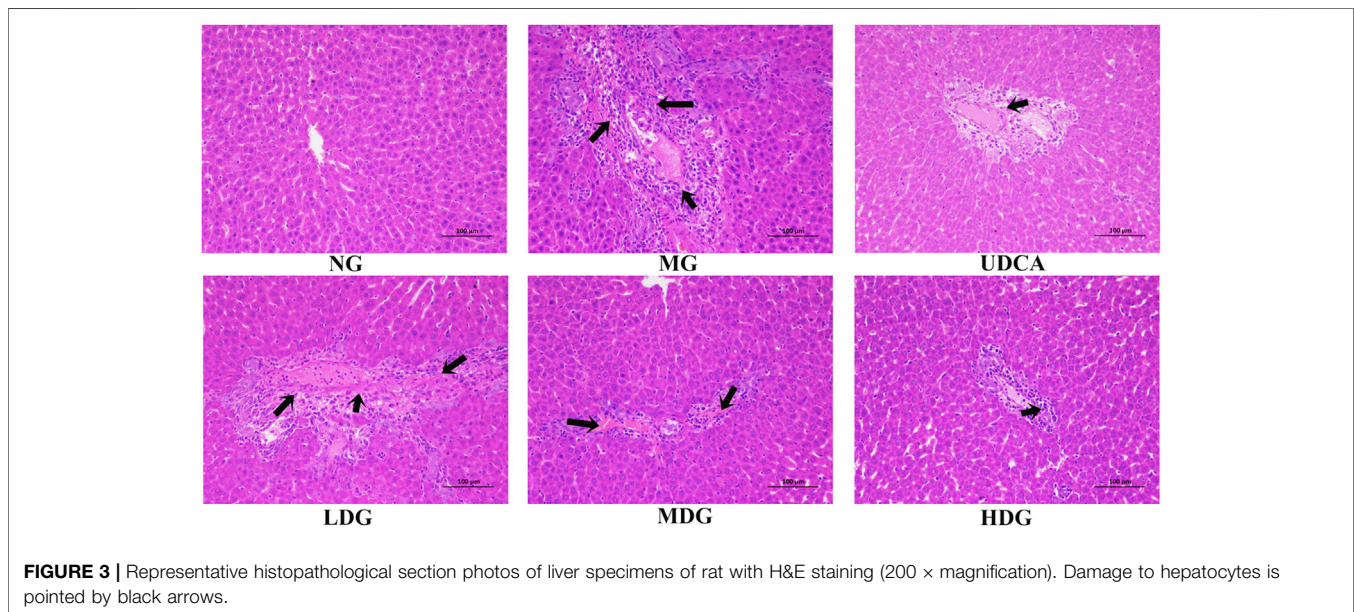
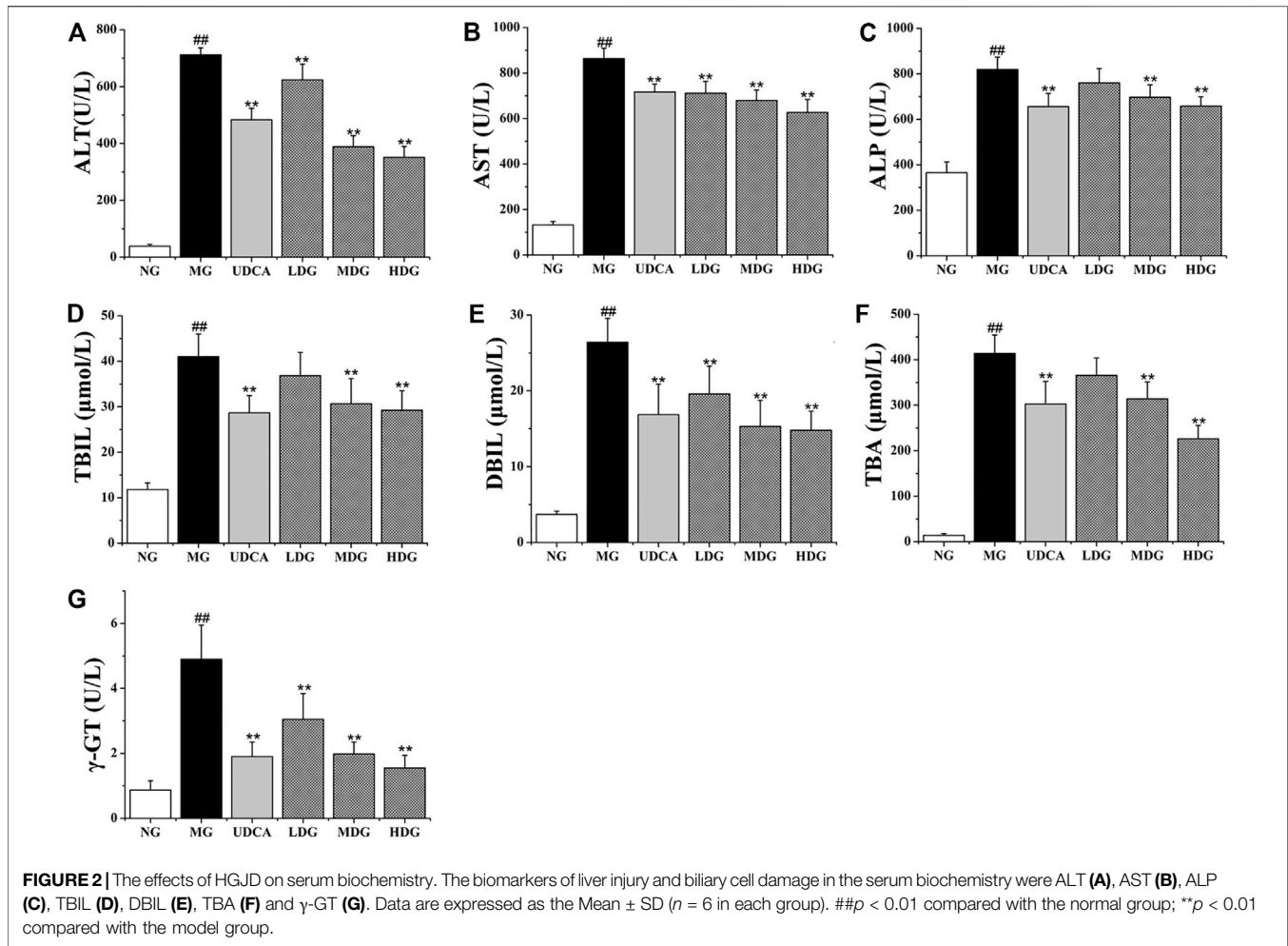


TABLE 1 | Characterization of serum migrant compounds of HGJD by UPLC-Q-Exactive MS/MS.

NO.	Compound	RT (min)	Formula	Precursor ion	Predictived	Measured	Error (ppm)	MS2	Source	Reference
S1	Acetophenone	1.88	C ₈ H ₈ O	[M + H] ⁺	121.0647	121.0652	4.13	103.0539, 91.0548, and 53.0391	CP	Zheng et al. (2020)
S2	Quinic acid	1.94	C ₇ H ₁₂ O ₆	[M-H] ⁻	191.0561	191.0559	-1.05	173.0453, 85.0285	ZZ	Zhou et al. (2020)
S3	Nicotinamide	2.46	C ₆ H ₆ N ₂ O	[M + H] ⁺	123.0552	123.0554	1.63	88.0236, 80.0500, 56.9654, and 53.0392	CP	Zheng et al. (2020)
S4	Citric acid	3.23	C ₆ H ₈ O ₇	[M-H] ⁻	191.0197	191.0195	-1.05	111.0080, 87.0078	BS	Xu et al. (2018)
S5	Geniposidic acid	4.67	C ₁₆ H ₂₂ O ₁₀	[M-H] ⁻	373.114	373.1147	1.88	211.0611, 167.070, 123.0444, and 149.0602	ZZ	Wang et al. (2016)
S6	Shanzhiside	4.71	C ₁₆ H ₂₄ O ₁₁	[M-H] ⁻	391.1245	391.1254	2.30	193.0507	ZZ	Zhou et al. (2020)
S7	Gardenoside	5.64	C ₁₇ H ₂₄ O ₁₁	[M-H] ⁻	403.1245	403.1274	7.19	241.0719	ZZ	Fu et al. (2014)
S8	Jasminoside B	6.47	C ₁₆ H ₂₆ O ₈	[M + H] ⁺	347.17	347.1700	0	185.1172, 167.1066	ZZ	Zhou et al. (2020)
S9	Methyl gallate	6.63	C ₈ H ₆ O ₅	[M-H] ⁻	183.0298	183.0296	-1.09	168.0059, 124.0158	BS MDP	Li et al. (2018)
S10	Oxypaeoniflorin	7.02	C ₂₃ H ₂₈ O ₁₂	[M-H] ⁻	495.1508	495.1514	1.21	165.0555	BS MDP	Zhan et al. (2018)
S11	Chlorogenic acid*	7.66	C ₁₆ H ₁₈ O ₉	[M + H] ⁺	355.1023	355.1022	-0.28	—	ZZ	Wang et al., 2016; Zhou et al. (2020)
S12	Geniposide*	8.01	C ₁₇ H ₂₄ O ₁₀	[M + H] ⁺	389.1442	389.1446	1.03	—	ZZ	Zhou et al. (2020)
S13	Peimisine	8.27	C ₂₇ H ₄₁ NO ₃	[M + H] ⁺	428.3159	428.3157	-0.47	67.0549, 84.0813, 81.0704, and 79.0550	ZBM	Zhou et al. (2013)
S14	Peimine*	8.35	C ₂₇ H ₄₅ NO ₃	[M + H] ⁺	432.3472	432.3470	-0.46	414.3004, 95.0860, and 67.0548	ZBM	Wang et al. (2014)
S15	Peiminine*	8.71	C ₂₇ H ₄₃ NO ₃	[M + H] ⁺	430.3315	430.3313	-0.46	412.3204, 98.0967	ZBM	Zhou et al. (2013)
S16	Albiflorin*	8.78	C ₂₃ H ₂₈ O ₁₁	[M-H] ⁻	525.1613	525.1619	1.28	357.1193, 121.0287	BS	Qi et al., 2014; Xiang et al. (2016)
S17	Paeoniflorin*	9.23	C ₂₃ H ₂₈ O ₁₁	[M-H] ⁻	525.1613	525.1621	1.52	449.1466, 327.1079, 165.0550, and 121.0300	BS,MDP	Qi et al. (2014)
S18	Ebeiedinone	10.32	C ₂₇ H ₄₃ NO ₂	[M + H] ⁺	414.3366	414.3364	-0.48	67.0548, 81.070, 91.0547, 93.0702, 105.0702, and 119.0857	ZBM	Zhou et al. (2013)
S19	Isoquercitrin	10.48	C ₂₁ H ₂₀ O ₁₂	[M + H] ⁺	465.1027	465.1032	1.08	303.0497	CP,ZZ	Fu et al. (2014); Zhang et al. (2018)
S20	Puqiedinone	10.63	C ₂₇ H ₄₃ NO ₂	[M + H] ⁺	414.3366	414.3359	-1.69	105.0702, 91.0547, 81.0704, 67.0548, and 55.0549	ZBM	Zhou et al. (2013)
S21	Narirutin*	10.90	C ₂₇ H ₃₂ O ₁₄	[M + H] ⁺	581.1864	581.1855	-1.55	273.0750, 153.0181	CP,QP	Zheng et al. (2019)
S22	Hesperetin	11.43	C ₁₆ H ₁₄ O ₆	[M + H] ⁺	303.0863	303.0859	-1.32	219.0640, 171.0288, 153.0181, 135.0439, 89.0390, and 67.0185	CP,QP	Zheng et al. (2020)
S23	Galloylpaeoniflorin	11.43	C ₃₀ H ₃₂ O ₁₅	[M + H] ⁺	633.1814	633.1783	-4.90	153.0184	BS,MDP	(Xiang et al., 2016; Zhan et al., 2018)
S24	Hesperidin*	11.45	C ₂₈ H ₃₄ O ₁₅	[M-H] ⁻	609.1824	609.1832	1.31	301.0719, 286.0480	CP,QP	(Xu et al., 2018; Zheng et al., 2019)
S25	Didymin*	13.90	C ₂₈ H ₃₄ O ₁₄	[M + H] ⁺	595.2021	595.2021	0	287.0908	CP,QP	Tong et al. (2018)
S26	Naringenin	16.85	C ₁₅ H ₁₂ O ₅	[M-H] ⁻	271.0611	271.0615	1.48	151.0041	CP,QP	Zheng et al. (2019)
S27	Paeonol*	19.10	C ₉ H ₁₀ O ₃	[M + H] ⁺	167.0702	167.0701	-0.60	149.0596, 121.0648	BS,MDP	Xu et al. (2018)
S28	Nobiletin*	20.71	C ₂₁ H ₂₂ O ₈	[M + H] ⁺	403.1387	403.1383	-0.99	403.1383, 388.1152, and 373.0914	CP,QP	Cai et al. (2019)
S29	Hepta-3*	21.72	C ₂₂ H ₂₄ O ₉	[M + H] ⁺	433.1493	433.1489	-0.92	418.1256, 403.1018, and 385.0910	CP,QP	Cai et al. (2019)

(Continued on following page)

TABLE 1 | (Continued) Characterization of serum migrant compounds of HGJD by UPLC-Q-Exactive MS/MS.

NO.	Compound	RT (min)	Formula	Precursor ion	Predictived	Measured	Error (ppm)	MS2	Source	Reference
S30	Tangeretin	22.45	C ₂₀ H ₂₀ O ₇	[M + H] ⁺	373.1281	373.1276	-1.34	373.1280, 343.0809	CP,QP	Xu et al. (2018)
S31	Alisol B	25.97	C ₃₀ H ₄₈ O ₄	[M + H] ⁺	473.3625	473.3626	0.21	437.342	ZX	Li et al. (2017)

CP, *Citri Reticulatae Pericarpium* (*Citrus reticulata* Blanco); QP, *Citri Reticulatae Pericarpium Viride* (*Citrus reticulata* Blanco); BS, *Paeoniae Radix Alba* (*Paeonia lactiflora* Pall); MDP, *Moutan Cortex* (*Paeonia suffruticosa* Andr.); ZZ, *Gardeniae Fructus* (*Gardenia jasminoides* Ellis); ZX, *Alismatis Rhizaoma* (*Alisma plantago-aquatica* Linn.); ZBM, *Fritillariae Thunbergii Bulbus* (*Fritillaria thunbergii* Miq.).

The substances with * in the table have been compared with the reference substance.

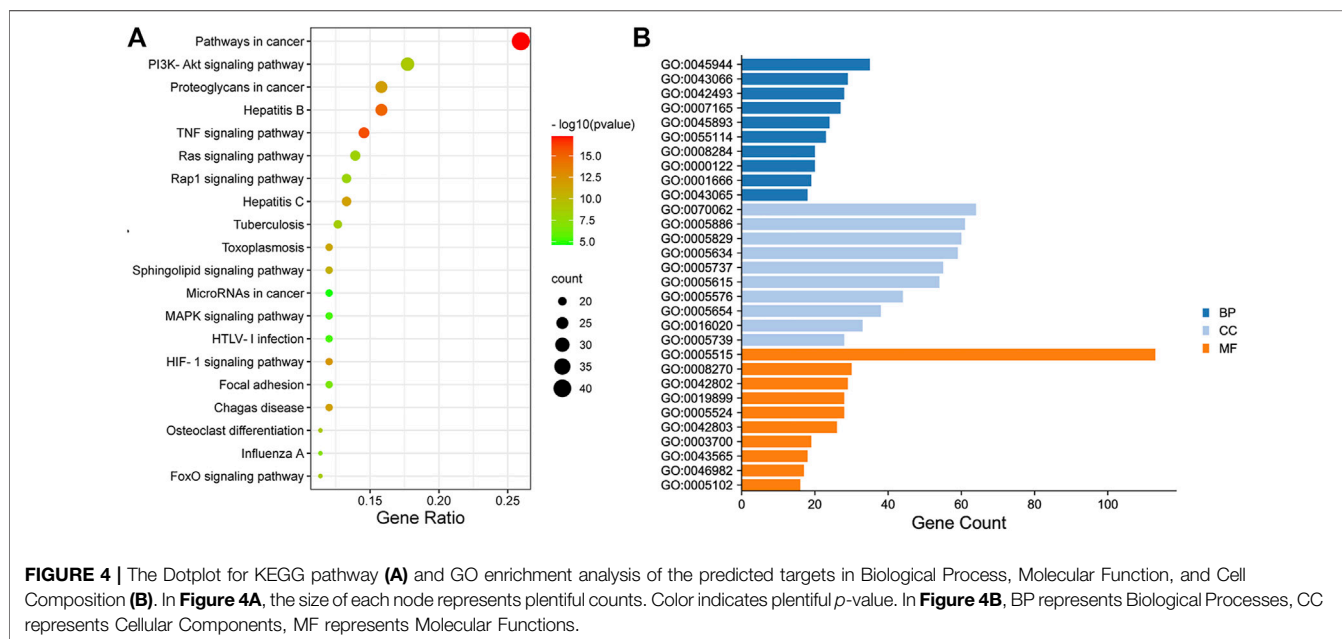


FIGURE 4 | The Dotplot for KEGG pathway (A) and GO enrichment analysis of the predicted targets in Biological Process, Molecular Function, and Cell Composition (B). In **Figure 4A**, the size of each node represents plentiful counts. Color indicates plentiful *p*-value. In **Figure 4B**, BP represents Biological Processes, CC represents Cellular Components, MF represents Molecular Functions.

following pathways: pathways in cancer, PI3K-Akt signaling pathway and hepatitis B, *etc.*

The top10 results enriched by GO were displayed in **Figure 4B**; **Supplementary Table S4**. It was found that the target genes were involved in Cellular Components (CC), including extracellular exosome, plasma membrane, cytosol, and nucleus, *etc.* As for Biological Processes (BP), the key genes were mainly concentrated in negative regulation of apoptotic process, response to drug, signal transduction, and oxidation-reduction process. These functions closely correlated with protein binding, zinc ion binding, enzyme binding, and ATP binding in Molecular Functions (MF).

3.3.3 Network Construction

Drug-components-targets network was conducted based on 31 serum migrant compounds of HGJD and 159 targets with therapeutic potential. (**Supplementary Figure S3A**; **Supplementary Table S5**). Besides, the protein-protein interaction network was established to screen the key targets of HGJD against CHI. As shown in

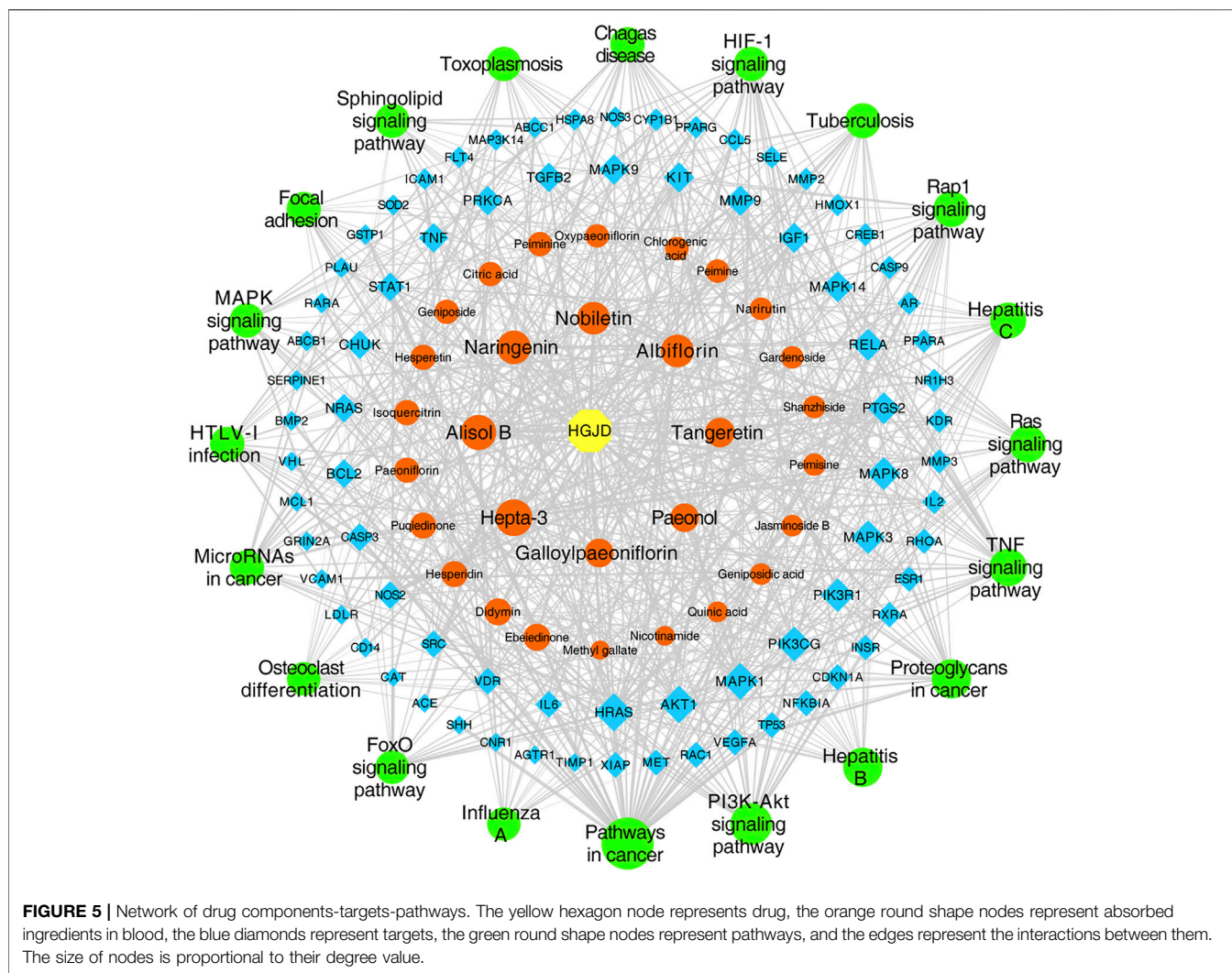
Supplementary Figure S3B, the key targets involving in the anti-CHI effects of HGJD included MAPK1, AKT, MAPK3, and PIK3R1.

The top 20 signaling pathways enriched by KEGG, targets involved in the top 20 signaling pathways, and the corresponding ingredients in HGJD were submitted to Cytoscape 3.7.1 to construction of the components-targets-pathways network (**Figure 5**). The network was consisted of 127 nodes (including 1 drug, 30 serum migrant compounds, 76 targets, and 20 pathways) and 728 edges. In addition, the network analysis result indicated that serum migrant compounds which had high degree value include hepta-3, alisol B, naringenin, nobiletin, albiflorin, tangeretin, paeonol, and galloylpaeoniflorin, might be the potential active ingredients of HGJD treating CHI.

3.4 Metabolomics

3.4.1 Multivariable Data Analysis

The typically based peak intensity chromatograms of serum samples in different groups were shown in **Supplementary Figure S4**, **S5**. Meanwhile, QC samples could cluster



together, indicating that the instrument was stable (**Supplementary Figure S6**). The PCA and PLS-DA score plots (ESI+: $R2X = 0.435$, $R2Y = 0.994$, and $Q2 = 0.898$; ESI-: $R2X = 0.480$, $R2Y = 0.997$, and $Q2 = 0.92$) indicated that the normal group, model group and high dose of HGJD treatment group were separated from each other (**Figures 6A–D**), the combination of histological and biochemical examination confirmed the reliability of the CHI model and reflected the regulatory effect of HGJD on metabolites. Simultaneously, permutation test indicated that PLS-DA model was not over-fitted. (**Figures 6E,F**). The complexity of the model was reduced using OPLS-DA and the interpretation of the model was improved (**Figures 6G,H**). The results showed that the metabolites in each group have achieved complete separation (ESI+: $R2X = 0.372$, $R2Y = 0.999$, $Q2 = 0.859$; ESI-: $R2X = 0.356$, $R2Y = 0.985$, and $Q2 = 0.901$) in two ion modes. Further, VIP value in OPLS-DA was one of the important factors for identifying differential metabolites.

3.4.2 Identification of Differential Biomarkers

OPLS-DA models and *t*-test were applied to distinguish the differential metabolites induced by ANIT and improved by HGJD. Differential biomarkers were screened by a criterion of p -value < 0.05 and $VIP > 1$. Based on literature reports and four online databases including Human Metabolome Database (HMDB) (<http://www.hmdb.ca>), Metlin (<http://metlin.scripps.edu>), massbank (<http://www.massbank.jp/>), LipidMaps (<http://www.lipidmaps.org>), and mzcloud (<https://www.mzcloud.org>), the differential biomarkers were tentatively identified. In total, 16 differential metabolites were screened out. As shown in **Table 2**, 7 metabolites were up-regulated and 9 metabolites were down-regulated with ANIT intervention in model group. Compared to this trend, the level of 13 metabolites was significantly reversed ($p < 0.05$) in the high dose of HGJD treatment group. The heatmap of 16 biomarkers was displayed in **Figure 7**, which demonstrated that ANIT treatment could influence the level of endogenous metabolites notably, while HGJD treatment had beneficial effects for the recovery of metabolite disorders.

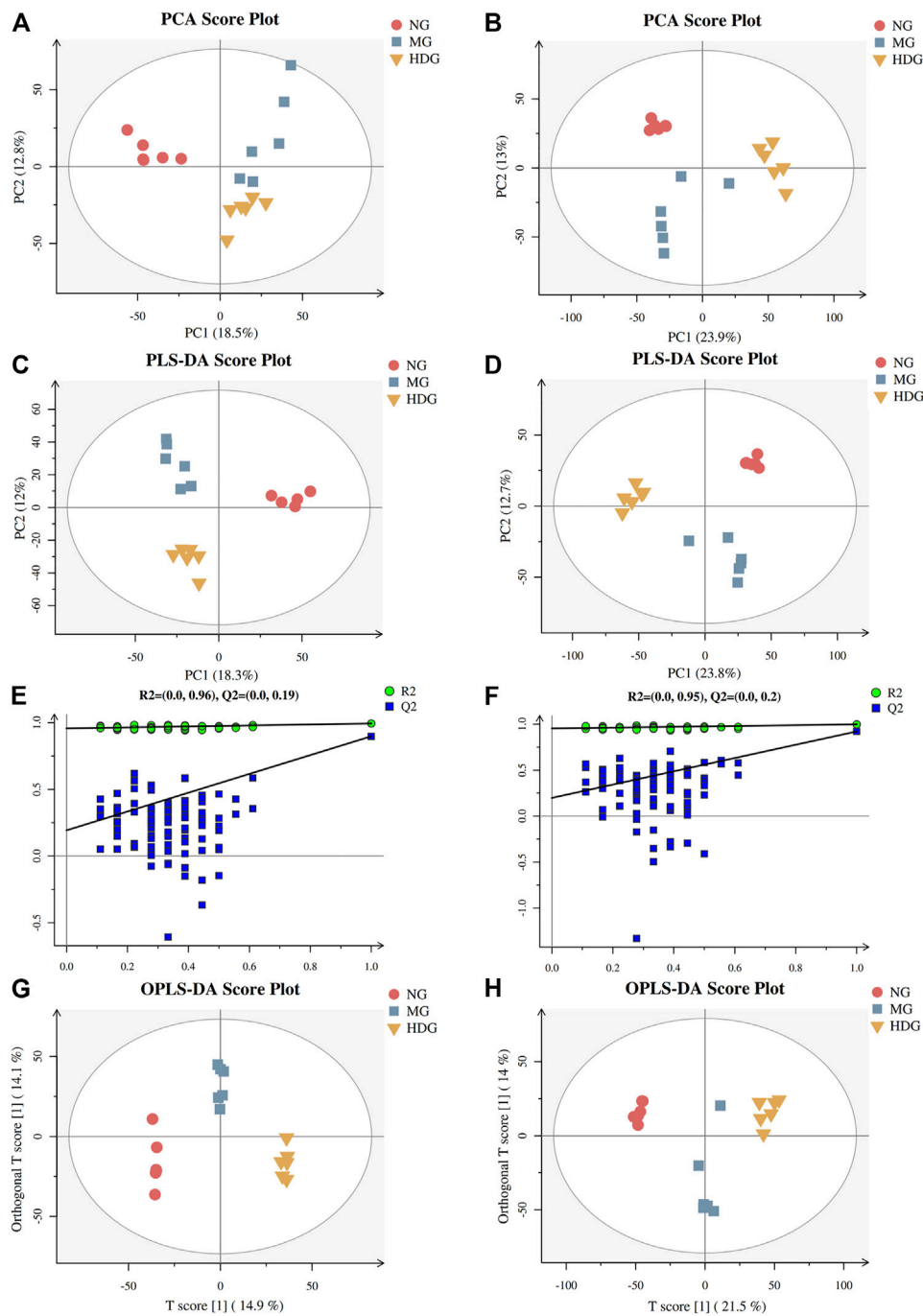


FIGURE 6 | The results of multivariate statistical analysis. The PCA score graph in positive (A) and negative (B) ion mode. The PLS-DA score graph in positive (C) and negative (D) ion mode. Permutations graph in positive (E) and negative (F) ion mode. The OPLS-DA score graph in positive (G) and negative (H) ion mode.

3.4.3 Metabolic Pathway Analysis

Metabolic pathway analysis was carried out to explore the underlying molecular functions of these serum differential metabolites. The result revealed that 5 pathways were affected by the administration of HGJD, including primary bile acid biosynthesis, tyrosine metabolism, pentose phosphate pathway,

glutathione metabolism and glycerophospholipid metabolism (Figure 8; Table 3).

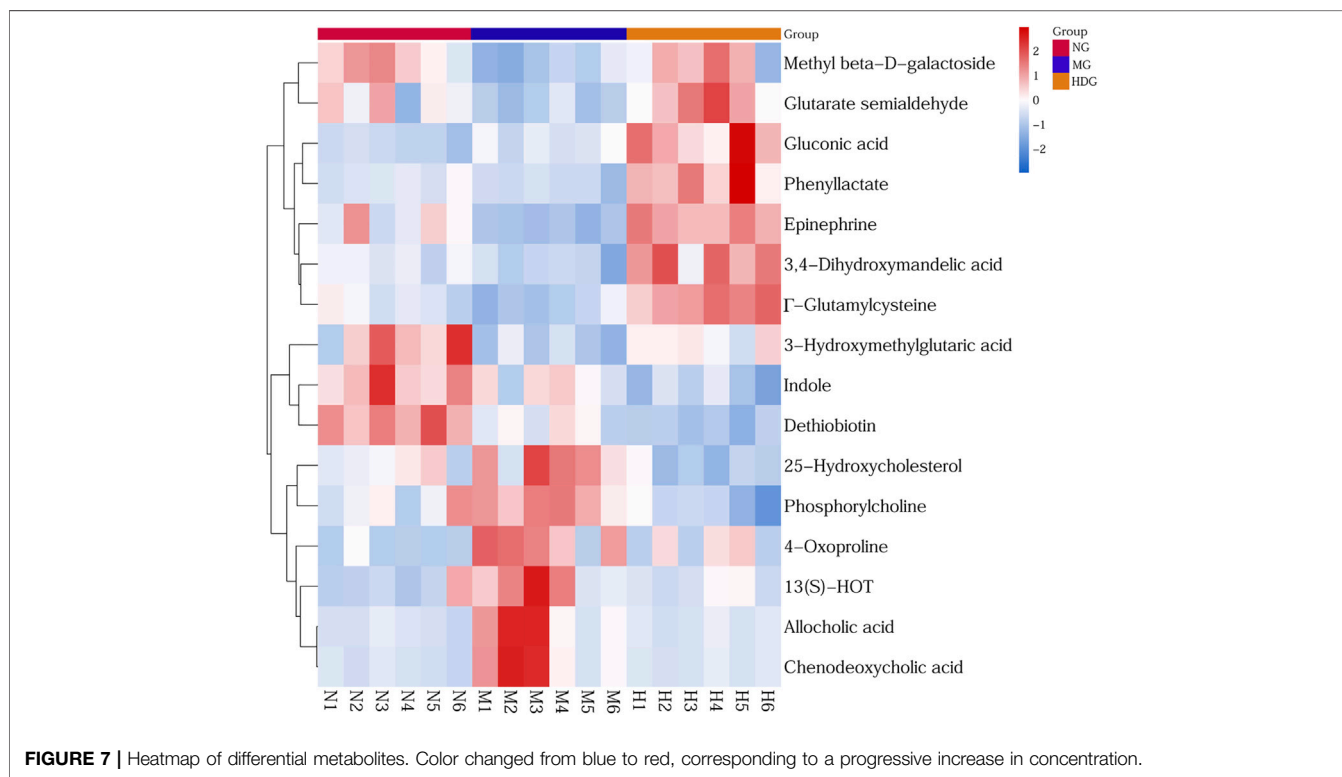
3.4.4 Signaling Networks

We imported the identified differential metabolites into the KEGG (<http://www.kegg.jp/>) to find signaling pathways

TABLE 2 | List and change trends of differential metabolites in the rats serum induced by ANIT.

No	Name	RT(min)	Formula	Exact mass	Error (ppm)	KEGG	Type	Trend	
								MG vs NG	HDG vs MG
1	Methyl beta-D-galactoside	0.69	C ₇ H ₁₄ O ₆	194.0790	6.69	C03619	[M + H] ⁺	↓	↑
2	Epinephrine	1.03	C ₉ H ₁₃ NO ₃	183.0895	12.25	C00788	[M + H] ⁺	↓	↑
3	3-Hydroxymethylglutaric acid	1.10	C ₆ H ₁₀ O ₅	162.0528	8.96	C03761	[M-H] ⁻	↓	↑
4	Gluconic acid	1.27	C ₆ H ₁₂ O ₇	196.0583	2.79	C00257	[M-H] ⁻	↑	↑
5	Glutarate semialdehyde	2.81	C ₅ H ₈ O ₃	116.0473	14.90	C03273	[M-H] ⁻	↓	↑
6	3,4-Dihydroxymandelic acid	2.97	C ₈ H ₈ O ₅	184.0370	3.54	C05580	[M-H] ⁻	↓	↑
7	Indole	3.02	C ₈ H ₇ N	117.0578	4.05	C00463	[M + H] ⁺	↓	↓
8	Phenyllactate	4.18	C ₉ H ₁₀ O ₃	166.0630	5.06	C05607	[M-H] ⁻	↓	↑
9	25-Hydroxycholesterol	5.62	C ₂₇ H ₄₆ O ₂	402.3498	2.56	C15519	[M-H] ⁻	↑	↓
10	Allocholic acid	6.14	C ₂₄ H ₄₀ O ₅	408.2876	7.46	C00695	[M + H] ⁺	↑	↓
11	Chenodeoxycholic acid	6.14	C ₂₄ H ₄₀ O ₄	392.2927	15.10	C02528	[M + H] ⁺	↑	↓
12	Dethiobiotin	6.54	C ₁₀ H ₁₈ N ₂ O ₃	214.1317	11.18	C01909	[M-H] ⁻	↓	↓
13	Phosphorylcholine	7.27	C ₅ H ₁₅ NO ₄ P	184.0739	1.02	C00588	[M + H] ⁺	↑	↓
14	4-Oxoproline	8.57	C ₅ H ₇ NO ₃	129.0426	1.54	C01877	[M + H] ⁺	↑	↓
15	13(S)-HOT	8.65	C ₁₈ H ₃₀ O ₃	294.2195	1.04	C16316	[M + H] ⁺	↑	↓
16	Γ-Glutamylcysteine	9.63	C ₈ H ₁₄ N ₂ O ₅ S	250.0623	0.97	C00669	[M-H] ⁻	↓	↑

↑: Compound is up-regulated. ↓: Compound is down-regulated.



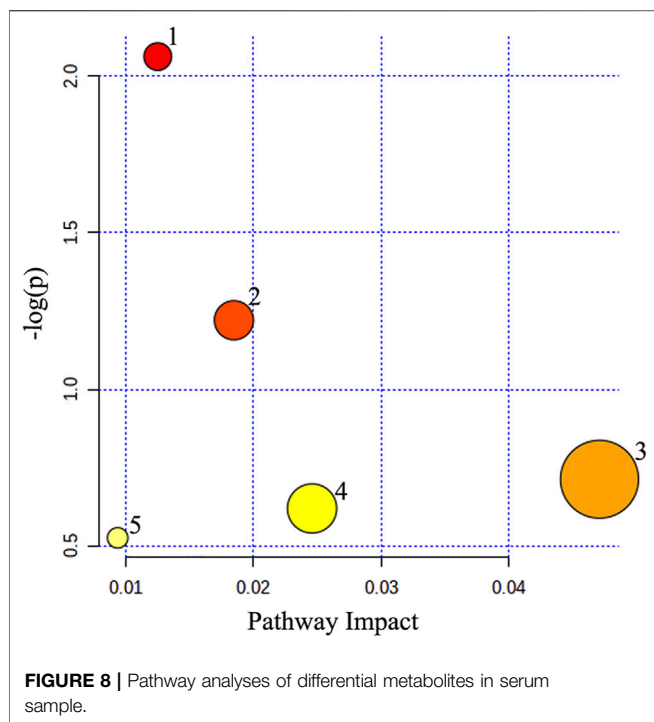
correlated with them. Moreover, relationships among different signaling pathways were analyzed based on literatures. As shown in **Figure 9**, primary bile acid biosynthesis, tyrosine metabolism and glutathione metabolism might be related to the anti-CHI effect of HGJD. Meanwhile, when compared with model group, the levels of 25-Hydroxycholesterol, cholic acid, and chenodeoxycholic acid were significantly down-regulated by HGJD. Conversely, the levels of Γ-Glutamylcysteine,

Epinephrine and 3, 4-Dihydroxymandelic acid were significantly increased by HGJD.

3.5 Regulation of PI3K/Akt/Nrf2 Pathway

3.5.1 Western Blotting Assay

Integrating liver biochemistry, network analysis and metabolomics results, PI3K/Akt pathway, primary bile acid biosynthesis as well as secretion, and glutathione metabolism



might be involved in the anti-CHI effect of HGJD. Meanwhile, accumulated evidence has shown that activation of PI3K/Akt pathway could induce nuclear translocation of Nrf2, and then affect GSH synthesis, which was an important mechanism of nature product protection against hepatic oxidative injury (Ma et al., 2015; Jin et al., 2019; Mukherjee et al., 2021). Therefore, western blotting was used to test and verify the effect of HGJD on PI3K/Akt/Nrf2 signaling pathway. As displayed in **Figure 10**, the protein expressions of PI3K, p-Akt, Nrf2, GCLC, and GCLM were decreased in ANIT induced model group. Whereas, these reduced protein levels were significantly increased after the treatment with HGJD.

3.5.2 Biochemical Analysis of Antioxidant Compounds in Liver Tissue

As reported in literatures, activation of PI3K/Akt/Nrf2 pathway could promote the imbalance between antioxidant system and oxidative system, which was closely related to mitigation of oxidative stress-induced injuries (Shi et al., 2018). Antioxidant compounds content (GSH, SOD) which could scavenge ROS, were significantly reduced with treatment of ANIT ($p < 0.01$). In

UDCA group, medium dose and high dose of HGJD group, the levels of these compounds in liver were significantly reversed, while the antioxidant effect of low dose of HGJD was weak (**Figures 11A,C**). The hepatic MDA which was one of oxidative stress products was significantly increased in the model group ($p < 0.01$). The treatment with different dose of HGJD significantly reversed the increase of MDA induced by ANIT (**Figure 11B**). These results demonstrated that the potential mechanism of HGJD to alleviate CHI might correlate with the activation of PI3K/Akt/Nrf2 pathway to induce antioxidant synthesis.

4 DISCUSSION

In this study, HGJD significantly decreased the biochemical indicators which were related to CHI, and improved the inflammatory infiltration induced by ANIT. The results suggested that HGJD had a protective effect against ANIT-induced CHI. In terms of biochemical results, the effect of HGJD was not as good as UDCA, which might be related to overall regulation, slowness, and long-lasting characteristics of TCM treatment. In addition, serum pharmacology combined with network analysis was applied to analyze drug-target interactions and identify potentially active components of HGJD. Moreover, mechanisms of anti-CHI effect of HGJD were explored by integrating network analysis and metabolomics, and the predicted main pathway was validated in the level of molecular biology. Although dosage in our study is within the range stipulated by Chinese Pharmacopoeia (2020 Edition), it is still larger than the dosage recommends for animal studies (Heinrich et al., 2020). Further pharmacological and toxicological studies are needed to guide the determination of clinical dose range.

Through literature research, we found that metabolic enzyme activity and gut microbiota might change under disease conditions, which could affect the absorption of pharmaceutical ingredients (Feng et al., 2020; Kummel and Hov, 2019; Pang et al., 2017; Qi et al., 2020). Therefore, in this experiment, the ANIT-induced CHI rats were selected to study serum pharmacology, so as to better reflect absorption of HGJD components under the pathological state of CHI. Moreover, the network analysis was used to screen for potential active components of HGJD. The present results showed that hepta-3, alisol B, naringenin, nobiletin, albiflorin, tangeretin, paeonol, and galloylpaeoniflorin were the pivotal compounds of the compound-target network of HGJD against CHI. As reported in literature, hepta-3, naringenin, tangeretin,

TABLE 3 | Results of metabolic pathway analysis.

No	Pathway name	Total	Hits	p-value	-log(p)	Impact
1	Primary bile acid biosynthesis	46	3	0.008671	2.0619	0.0125
2	Tyrosine metabolism	42	2	0.060225	1.2202	0.0185
3	Pentose phosphate pathway	22	1	0.193790	0.7127	0.0471
4	Glutathione metabolism	28	1	0.240200	0.6194	0.0246
5	Glycerophospholipid metabolism	36	1	0.298210	0.5255	0.0094

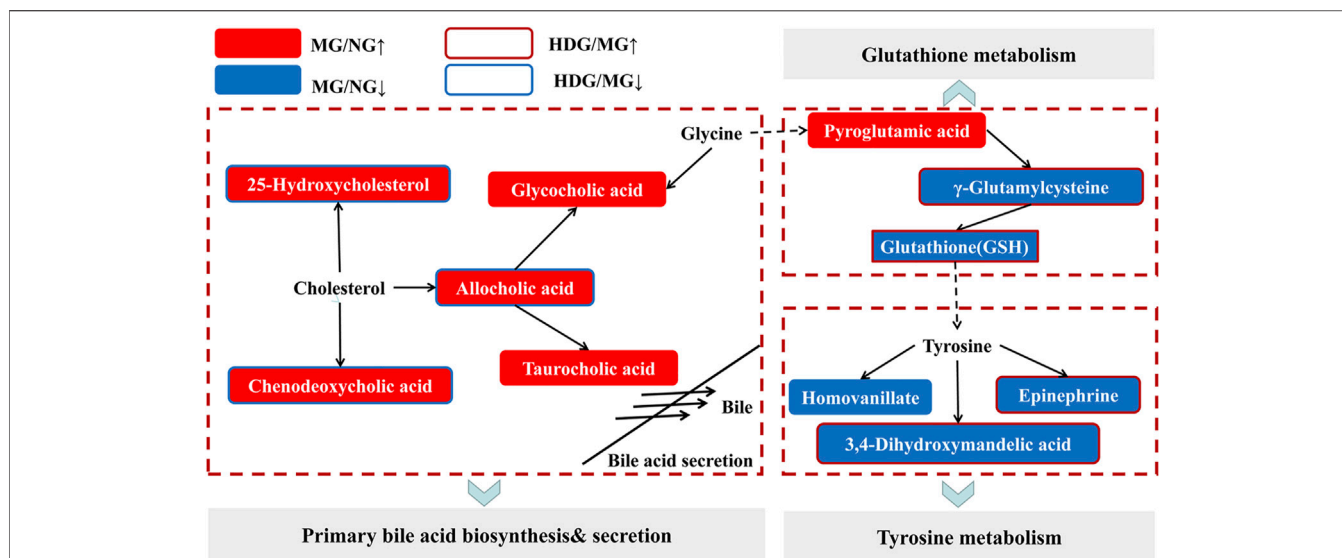


FIGURE 9 | Sketch map of the metabolic pathway correlated with CHI and HGJD therapy. The red and blue solid boxes represent that metabolites were significantly elevated or reduced in the model group when contrasted with normal group, respectively. The boxes with red and blue border indicated that metabolites were significantly increased or decreased in the HGJD group when compared with model group, respectively.

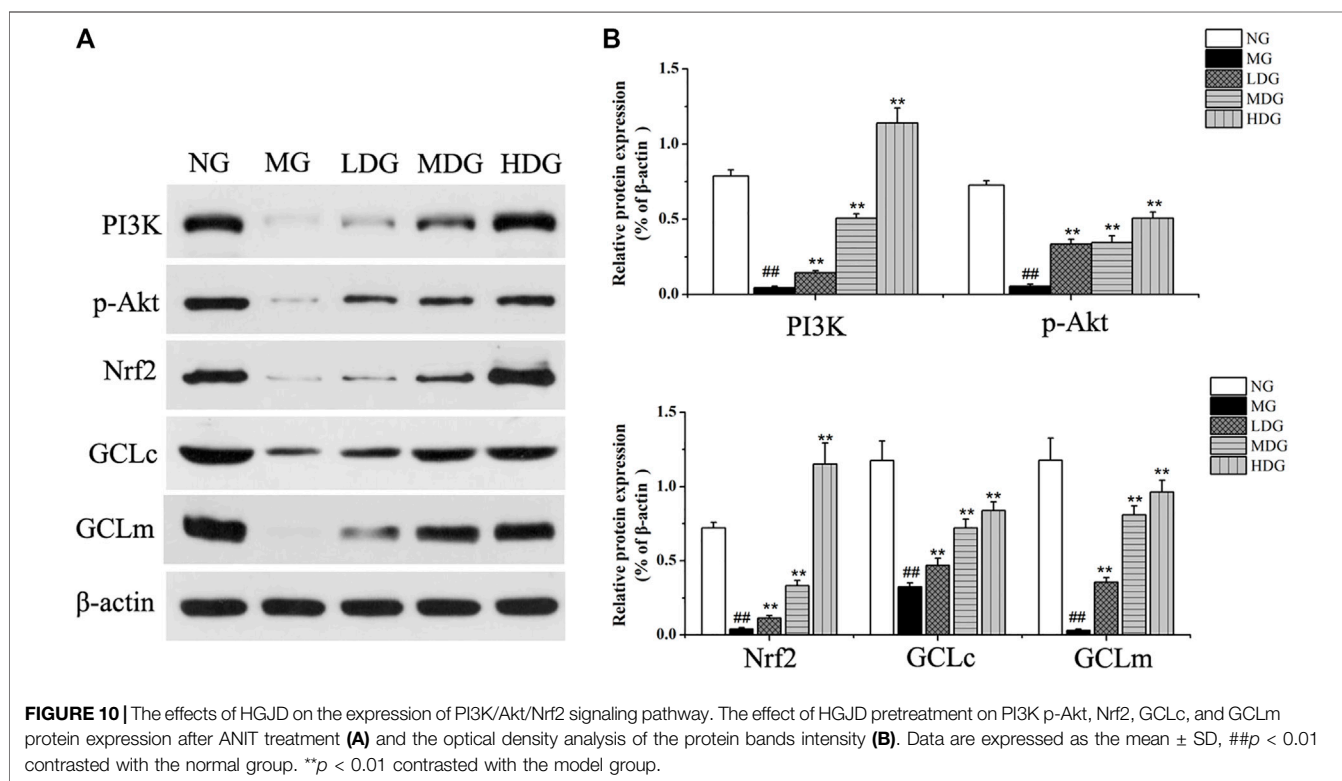
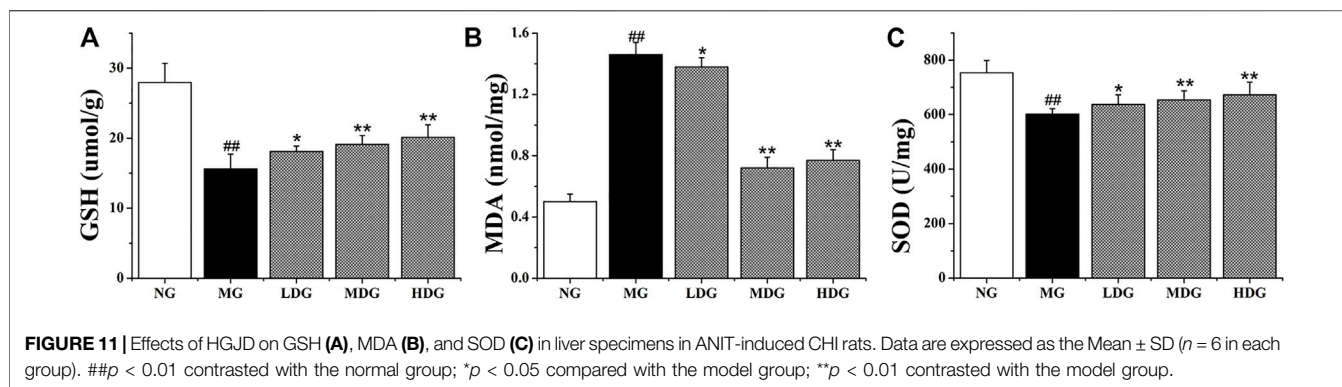


FIGURE 10 | The effects of HGJD on the expression of PI3K/Akt/Nrf2 signaling pathway. The effect of HGJD pretreatment on PI3K p-Akt, Nrf2, GCLc, and GCLm protein expression after ANIT treatment (A) and the optical density analysis of the protein bands intensity (B). Data are expressed as the mean ± SD, ##*p* < 0.01 contrasted with the normal group. ***p* < 0.01 contrasted with the model group.

and nobiletin could reduce oxidative stress-induced liver injury by Nrf2 related pathway (Lin et al., 2019). Due to the regulation of transporters and enzymes mediated by FXR, Alisol B 23-acetate has shown the anti-CHI effect in animal experiment (Meng et al., 2015). Albiflorin was the one of the main active compounds of *Paeonia lactiflora* Pall against CHI (Jiang et al., 2012). Paeonol

could alleviate live injury via anti-inflammatory, anti-oxidative and anti-apoptosis activity (Ding et al., 2016; Gong et al., 2017). These active components and their mixtures might play a vital role in protecting effect of HGJD against ANIT-induced CHI. However, the relationships among those compounds were complex, which needed to be explored in future work.



Past work has shown that inhibition of PI3K/Akt pathway might aggravate liver damage (Han et al., 2010; Liu W et al., 2019). Besides, natural products have been demonstrated to have hepatoprotective activity via up-regulated the expression of Nrf2 by activating the PI3K/Akt pathway (Zhang et al., 2017). From the results of network analysis, PI3K/Akt signaling pathway had a significant correlation with the key targets identified in our study. Furthermore, as reported in literature, under acute and chronic liver disease conditions, Nrf2 was activated and relieved oxidative stress-induced injuries by regulating genes expression of cytoprotective enzymes, which promoted GSH synthesis, and inhibited ROS generation (Bataille and Manautou, 2012; Xu et al., 2019). Based on our serum metabolomics research, glutathione metabolism might contribute to the anti-CHI effect of HGJD. Thus integrating results from network analysis and metabolomics showed that PI3K/Akt/Nrf2 signaling pathway related to glutathione (GSH) synthesis might be one of the major pathways interrelated to anti-CHI function of HGJD. Therefore, we further studied the connection among GSH synthesis, Nrf2 expression, and PI3K/Akt signaling pathways. As demonstrated in this study, HGJD could improve the protein expressions of PI3K, p-Akt, Nrf2, GCLc and GCLm, and increase GSH and SOD content. The results effectively corroborated the above prediction results, suggested that this integrated strategy was feasible.

As for CHI, excessive accumulation of bile acids in liver and systemic circulation could induce live cell damage (Gonzalez-Sanchez et al., 2016), which was related to bile acid-induced initiation of apoptosis and oxidative stress increase in liver cells (Sokolovic et al., 2013). The non-targeted metabolomics in our research showed that the therapeutic effect of HGJD was correlated with primary bile acid biosynthesis as well as secretion, and glutathione metabolism. Moreover, as reported in literature, farnesoid X receptor (FXR) played an important role in regulating bile acid. Meanwhile, oxidative stress in FXR-null mice increased spontaneously, which might be attributed to the continuous increase in hepatic bile acids level (Nomoto et al., 2009). However, there was a complex network of biological signaling pathways, and might be a clear tissue-specific role of FXR in the liver and intestine (Cheng, et al., 2021; Stofan and

Guo, 2020). FXR and the molecular mechanism by which it regulates bile acid and oxidative stress are valuable for further research.

In conclusion, this study showed that HGJD could alleviate CHI. A comprehensive method based on network analysis, metabolomics and *in vivo* validation experiment was used to investigate the mechanism of HGJD in treatment of CHI. PI3K/Akt/Nrf2 signaling pathway related to GSH synthesis has been identified as the staple pathway correlated with the effects of HGJD against CHI. Totally, 31 compounds originated from HGJD have been identified in the serum sample. The pivotal compounds in the network analysis were predicted as potential active components. In the future, other signaling pathways predicted in our study should be investigate, and the potential active ingredients can be used to improve the quality control of HGJD.

DATA AVAILABILITY STATEMENT

The original contribution presented in the study are included in the article/**Supplementary Material**; further inquiries can be directed to the corresponding authors.

ETHICS STATEMENT

The animal study was reviewed and approved by The Animal Ethics Committee of Chengdu University of Traditional Chinese Medicine (Chengdu, China).

AUTHOR CONTRIBUTIONS

C-MF and WL designed the study. QD, Y-PJ, S-YS, and LP performed the experiments, JC, Z-PZ, Y-FZ, and W-QC recorded the experimental data. QD wrote the manuscript. QD and XY made the charts. WL, ZZ, and J-MZ reviewed and edited the manuscript. All authors have read and approved the manuscript.

FUNDING

This work was supported by the Sichuan Provincial Key Research and Development Program (No. 2020YFS0567); the National Natural Science Foundation of China (Grant Nos. 81403103, 82073994); the International Cooperation Project of Science and Technology Department of Sichuan Province (Grant No. 2018HH0122); Chengdu Science and Technology Bureau International Science and

Technology Cooperation Project (Grant No. 2017-GH02-00054-HZ).

SUPPLEMENTARY MATERIAL

The Supplementary Material for this article can be found online at: <https://www.frontiersin.org/articles/10.3389/fphar.2021.773957/full#supplementary-material>

REFERENCES

- Bataille, A. M., and Manautou, J. E. (2012). Nrf2: a Potential Target for New Therapeutics in Liver Disease. *Clin. Pharmacol. Ther.* 92 (3), 340–348. doi:10.1038/clpt.2012.110
- Cai, H., Xu, Y., Xie, L., Duan, Y., Zhou, J., Liu, J., et al. (2019). Investigation on Spectrum-Effect Correlation between Constituents Absorbed into Blood and Bioactivities of Baizhu Shaoyao San before and after Processing on Ulcerative Colitis Rats by UHPLC/Q-TOF-MS/MS Coupled with Gray Correlation Analysis. *Molecules* 24 (5), 940. doi:10.3390/molecules24050940
- Cai, S. Y., and Boyer, J. L. (2021). The Role of Bile Acids in Cholestatic Liver Injury. *Ann. Transl. Med.* 9 (8), 737. doi:10.21037/atm-20-5110
- Chen, Y. H., Lan, T., Li, J., Qiu, C. H., Wu, T., Gou, H. J., et al. (2012). *Gardenia Jasminoides* Attenuates Hepatocellular Injury and Fibrosis in Bile Duct-Ligated Rats and Human Hepatic Stellate Cells. *World J. Gastroenterol.* 18 (48), 7158–7165. doi:10.3748/wjg.v18.i48.7158
- Cheng, H., Liu, J., Tan, Y., Feng, W., and Peng, C. (2021). Interactions between Gut Microbiota and Berberine, a Necessary Procedure to Understand the Mechanisms of Berberine. *J. Pharm. Anal.* doi:10.1016/j.jpaha.2021.10.003
- Ding, Y., Li, Q., Xu, Y., Chen, Y., Deng, Y., Zhi, F., et al. (2016). Attenuating Oxidative Stress by Paeonol Protected against Acetaminophen-Induced Hepatotoxicity in Mice. *PLoS One* 11 (5), e0154375. doi:10.1371/journal.pone.0154375
- Dunn, W. B., Broadhurst, D., Begley, P., Zelena, E., Francis-McIntyre, S., Anderson, N., et al. (2011). Procedures for Large-Scale Metabolic Profiling of Serum and Plasma Using Gas Chromatography and Liquid Chromatography Coupled to Mass Spectrometry. *Nat. Protoc.* 6 (7), 1060–1083. doi:10.1038/nprot.2011.335
- Feng, W. W., Liu, J., Ao, H., Yue, S. J., and Peng, C. (2020). Targeting gut microbiota for precision medicine: Focusing on the efficacy and toxicity of drugs. *Theranostics* 10 (24), 11278–11301. doi:10.7150/thno.47289
- Fu, Z., Ling, Y., Li, Z., Chen, M., Sun, Z., and Huang, C. (2014). HPLC-Q-TOF-MS/MS for Analysis of Major Chemical Constituents of Yinchen-Zhizi Herb Pair Extract. *Biomed. Chromatogr.* 28 (4), 475–485. doi:10.1002/bmc.3057
- Gao, Y. F., Xia, W. Z., Xia, L., and Ouyang, R. (2019). Effect of Huaganjian on the Function of Hepatocytes and Activated Hepatic Stellate Cells. *Lishizhen Med. Mater. Med. Res.* 30 (12), 2879–2881.
- Gong, X., Yang, Y., Huang, L., Zhang, Q., Wan, R. Z., Zhang, P., et al. (2017). Antioxidation, Anti-inflammation and Anti-apoptosis by Paeonol in LPS/d-GalN-induced Acute Liver Failure in Mice. *Int. Immunopharmacol.* 46, 124–132. doi:10.1016/j.intimp.2017.03.003
- Gonzalez-Sanchez, E., Perez, M. J., Nytofte, N. S., Briz, O., Monte, M. J., Lozano, E., et al. (2016). Protective Role of Biliverdin against Bile Acid-Induced Oxidative Stress in Liver Cells. *Free Radic. Biol. Med.* 97, 466–477. doi:10.1016/j.freeradbiomed.2016.06.016
- Han, J. W., Zhan, X. R., Li, X. Y., Xia, B., Wang, Y. Y., Zhang, J., et al. (2010). Impaired PI3K/Akt Signal Pathway and Hepatocellular Injury in High-Fat Fed Rats. *World J. Gastroenterol.* 16 (48), 6111–6118. doi:10.3748/wjg.v16.i48.6111
- He, Y. Z. (2009). Observation on Curative Effect of 80 Cases of Chronic Cholecystitis Treated by Chinese and Western Medicine. *Guangming Tradit. Chin. Med.* 24 (10), 1959. doi:10.3969/j.issn.1003-8914.2009.10.078
- Heinrich, M., Appendino, G., Efferth, T., Fürst, R., Izzo, A. A., Kayser, O., et al. (2020). Best Practice in Research - Overcoming Common Challenges in Phytopharmacological Research. *J. Ethnopharmacol.* 246, 112230. doi:10.1016/j.jep.2019.112230
- Hirschfield, G. M., Mason, A., Luketic, V., Lindor, K., Gordon, S. C., Mayo, M., et al. (2015). Efficacy of Obeticholic Acid in Patients with Primary Biliary Cirrhosis and Inadequate Response to Ursodeoxycholic Acid. *Gastroenterology* 148 (4), 751–e8. doi:10.1053/j.gastro.2014.12.005
- Hohenester, S., and Beuers, U. (2017). Chronic Cholestatic Liver Diseases : Differential Diagnosis, Pathogenesis and Current Treatment in Adults. *Internist (Berl)* 58 (8), 805–825. doi:10.1007/s00108-017-0287-z
- Jiang, F., Zhao, Y., Wang, J., Wei, S., Wei, Z., Li, R., et al. (2012). Comparative Pharmacokinetic Study of Paeoniflorin and Albiflorin after Oral Administration of *Radix Paeoniae Rubra* in normal Rats and the Acute Cholestatic Hepatitis Rats. *Fitoterapia* 83 (2), 415–421. doi:10.1016/j.fitote.2011.12.009
- Jin, J., Zheng, C., Lin, L., Luo, D. S., Liu, Q. Z., and Liu, Q. (2007). Dose-effect Relationship of Protective Effect of Qingpi on Acute Carbon Tetrachloride Induced Liver Injury in Rats. *Lishizhen Med. Mater. Med. Res.* (12), 2977–2978. doi:10.3969/j.issn.1008-0805.2007.12.064
- Jin, Y., Huang, Z. L., Li, L., Yang, Y., Wang, C. H., Wang, Z. T., et al. (2019). Quercetin Attenuates Toosendanin-Induced Hepatotoxicity through Inducing the Nrf2/GCL/GSH Antioxidant Signaling Pathway. *Acta Pharmacol. Sin.* 40 (1), 75–85. doi:10.1038/s41401-018-0024-8
- Kowdley, K. V., Luketic, V., Chapman, R., Hirschfield, G. M., Poupon, R., Schramm, C., et al. (2018). A Randomized Trial of Obeticholic Acid Monotherapy in Patients with Primary Biliary Cholangitis. *Hepatology* 67 (5), 1890–1902. doi:10.1002/hep.29569
- Kummen, M., and Hov, J. R. (2019). The gut microbial influence on cholestatic liver disease. *Liver Int.* 39 (7), 1186–1196. doi:10.1111/liv.14153
- Li, C. R., Li, M. N., Yang, H., Li, P., and Gao, W. (2018). Rapid Characterization of Chemical Markers for Discrimination of *Moutan Cortex* and its Processed Products by Direct Injection-Based Mass Spectrometry Profiling and Metabolomic Method. *Phytomedicine* 45, 76–83. doi:10.1016/j.phymed.2018.04.003
- Li, D. (2021). Discussion on Clinical Application of Huagan Jian Based on Treatment of Liver Depression by Relief Therapy. *J. Guangzhou Univ. Tradit. Chin. Med.* 38 (04), 842–845. doi:10.13359/j.cnki.gzxbtcm.2021.04.035
- Li, S., Jin, S., Song, C., Jia, S., Zhang, Y., Feng, Y., et al. (2017). The Strategy for Establishment of the Multiple Reaction Monitoring Based Characteristic Chemical Profile of Triterpenes in *Alismatis Rhizoma* Using Two Combined Tandem Mass Spectrometers. *J. Chromatogr. A* 1524, 121–134. doi:10.1016/j.chroma.2017.09.057
- Lin, Z. H., Chan, Y. F., Pan, M. H., Tung, Y. C., and Su, Z. Y. (2019). Aged Citrus Peel (Chenpi) Prevents Acetaminophen-Induced Hepatotoxicity by Epigenetically Regulating Nrf2 Pathway. *Am. J. Chin. Med.* 47 (8), 1833–1851. doi:10.1142/S0192415X19500939
- Liu, L. F., Liang, H. Z., and Bin, J. P. (2019). Clinical Observation on Hyperthyroidism Liver Damage Treated with Therapy Integrated Traditional Chinese Medicine and Western Medicine. *J. Pract. Tradit. Chin. Med.* 35 (09), 1073–1075.
- Liu, W., Jing, Z. T., Xue, C. R., Wu, S. X., Chen, W. N., Lin, X. J., et al. (2019). PI3K/AKT Inhibitors Aggravate Death Receptor-Mediated Hepatocyte Apoptosis and Liver Injury. *Toxicol. Appl. Pharmacol.* 381, 114729. doi:10.1016/j.taap.2019.114729
- Ma, X., Zhao, Y. L., Zhu, Y., Chen, Z., Wang, J. B., Li, R. Y., et al. (2015). *Paeonia Lactiflora Pall.* Protects against ANIT-Induced Cholestasis by Activating Nrf2 via PI3K/Akt Signaling Pathway. *Drug Des. Devel. Ther.* 9, 5061–5074. doi:10.2147/DDDT.S90030
- Meng, Q., Chen, X. L., Wang, C. Y., Liu, Q., Sun, H. J., Sun, P. Y., et al. (2015). Alisol B 23-acetate Protects against ANIT-Induced Hepatotoxicity and Cholestasis, Due

- to FXR-Mediated Regulation of Transporters and Enzymes Involved in Bile Acid Homeostasis. *Toxicol. Appl. Pharmacol.* 283 (3), 178–186. doi:10.1016/j.taap.2015.01.020
- Mukherjee, S., Ghosh, S., Choudhury, S., Gupta, P., Adhikary, A., and Chattopadhyay, S. (2021). Pomegranate Polyphenols Attenuate Inflammation and Hepatic Damage in Tumor-Bearing Mice: Crucial Role of NF-Kb and the Nrf2/GSH Axis. *J. Nutr. Biochem.* 97, 108812. doi:10.1016/j.jnutbio.2021.108812
- Nair, A., Morsy, M. A., and Jacob, S. (2018). Dose Translation between Laboratory Animals and Human in Preclinical and Clinical Phases of Drug Development. *Drug Dev. Res.* 79 (8), 373–382. doi:10.1002/ddr.21461
- Nie, X., Pang, L., Jiang, H. J., Chen, Y., Wang, L., Wang, S. J., et al. (2020). Study on Specific Chromatogram and Content Determination of Multi-index Components about Material Reference of Classic Prescription of Huaganjian. *China Tradit. Herb Drugs* 51 (20), 5177–5186. doi:10.7501/j.issn.0253-2670.2020.20.009
- Nomoto, M., Miyata, M., Yin, S., Kurata, Y., Shimada, M., Yoshinari, K., et al. (2009). Bile Acid-Induced Elevated Oxidative Stress in the Absence of Farnesoid X Receptor. *Biol. Pharm. Bull.* 32 (2), 172–178. doi:10.1248/bpb.32.172
- Peng, H. Q., Tang, Y. P., Cao, Y. J., Tan, Y. J., Jin, Y., Shi, X. Q., et al. (2017). Comparatively evaluating the pharmacokinetic of fifteen constituents in normal and blood deficiency rats after oral administration of Xin-Sheng-Hua Granule by UPLC-MS/MS. *J. Chromatogr. B Analyt. Technol. Biomed. Life Sci.* 1061–1062, 372–381. doi:10.1016/j.jchromb.2017.07.042
- Pollock, G., and Minuk, G. Y. (2017). Diagnostic Considerations for Cholestatic Liver Disease. *J. Gastroenterol. Hepatol.* 32 (7), 1303–1309. doi:10.1111/jgh.13738
- Qi, Y., Cheng, X. H., Jing, H. T., Yan, T. X., Xiao, F., Wu, B., et al. (2020). Comparative pharmacokinetic study of the components in *Alpinia oxyphylla* Miq.-*Schisandra chinensis* (Turcz.) Baill. herb pair and its single herb between normal and Alzheimer's disease rats by UPLC-MS/MS. *J. Pharm. Biomed. Anal.* 177, 112874. doi:10.1016/j.jpba.2019.112874
- Qi, Y., Li, S., Pi, Z., Song, F., Lin, N., Liu, S., et al. (2014). Chemical Profiling of Wutou Decoction by UPLC-Q-TOF-MS. *Talanta* 118, 21–29. doi:10.1016/j.talanta.2013.09.054
- Shi, A., Shi, H., Wang, Y., Liu, X., Cheng, Y., Li, H., et al. (2018). Activation of Nrf2 Pathway and Inhibition of NLRP3 Inflammasome Activation Contribute to the Protective Effect of Chlorogenic Acid on Acute Liver Injury. *Int. Immunopharmacol.* 54, 125–130. doi:10.1016/j.intimp.2017.11.007
- Smith, C. A., Want, E. J., O'Maille, G., Abagyan, R., and Siuzdak, G. (2006). XCMS: Processing Mass Spectrometry Data for Metabolite Profiling Using Nonlinear Peak Alignment, Matching, and Identification. *Anal. Chem.* 78 (3), 779–787. doi:10.1021/ac051437y
- Sokolovic, D., Nikolic, J., Kocic, G., Jevtovic-Stoimenov, T., Veljkovic, A., Stojanovic, M., et al. (2013). The Effect of Ursodeoxycholic Acid on Oxidative Stress Level and DNase Activity in Rat Liver after Bile Duct Ligation. *Drug Chem. Toxicol.* 36 (2), 141–148. doi:10.3109/01480545.2012.658919
- Stofan, M., and Guo, G. L. (2020). Bile Acids and FXR: Novel Targets for Liver Diseases. *Front. Med. (Lausanne)* 7, 544. doi:10.3389/fmed.2020.00544
- Tong, C., Peng, M., and Shi, S. (2018). Rapid Identification of Flavonoid Compounds in *Pericarpium Citri Reticulatae* by Online Extraction-High Performance Liquid Chromatography-Diode Array Detection-Quadrupole Time-Of-Flight Mass Spectrometry. *Se. Pu.* 36 (3), 278–284. doi:10.3724/SP.J.1123.2017.11031
- Wang, G. W., Bao, B., Han, Z. Q., Han, Q. Y., and Yang, X. L. (2016). Metabolic Profile of *Fructus Gardeniae* in Human Plasma and Urine Using Ultra High-Performance Liquid Chromatography Coupled with High-Resolution LTQ-Orbitrap Mass Spectrometry. *Xenobiotica* 46 (10), 901–912. doi:10.3109/00498254.2015.1132793
- Wang, X., Shen, Y., Wang, S., Li, S., Zhang, W., Liu, X., et al. (2017). PharmMapper 2017 Update: a Web Server for Potential Drug Target Identification with a Comprehensive Target Pharmacophore Database. *Nucleic Acids Res.* 45 (W1), W356–w360. doi:10.1093/nar/gkx374
- Wang, Y., Zhang, S., Li, F., Zhou, Y., Zhang, Y., Wang, Z., et al. (2020). Therapeutic Target Database 2020: Enriched Resource for Facilitating Research and Early Development of Targeted Therapeutics. *Nucleic Acids Res.* 48 (D1), D1031–D1041. doi:10.1093/nar/gkz981
- Wang, Y., Li, C. M., Huang, L., Liu, L., Guo, Y. L., Ma, L., et al. (2014). Rapid Identification of Traditional Chinese Herbal Medicine by Direct Analysis in Real Time (DART) Mass Spectrometry. *Anal. Chim. Acta* 845, 70–76. doi:10.1016/j.aca.2014.06.014
- Xiang, H., Zhang, L., Song, J., Fan, B., Nie, Y., Bai, D., et al. (2016). The Profiling and Identification of the Absorbed Constituents and Metabolites of Guizhi Decoction in Rat Plasma and Urine by Rapid Resolution Liquid Chromatography Combined with Quadrupole-Time-Of-Flight Mass Spectrometry. *Int. J. Mol. Sci.* 17 (9), 1409. doi:10.3390/ijms17091409
- Xu, D., Xu, M., Jeong, S., Qian, Y., Wu, H., Xia, Q., et al. (2019). The Role of Nrf2 in Liver Disease: Novel Molecular Mechanisms and Therapeutic Approaches. *Front. Pharmacol.* 9, 1428. doi:10.3389/fphar.2018.01428
- Xu, Y., Cai, H., Cao, G., Duan, Y., Pei, K., Tu, S., et al. (2018). Profiling and Analysis of Multiple Constituents in Baizhu Shaoyao San before and after Processing by Stir-Frying Using UHPLC/Q-TOF-MS/MS Coupled with Multivariate Statistical Analysis. *J. Chromatogr. B Analyt. Technol. Biomed. Life Sci.* 1083, 110–123. doi:10.1016/j.jchromb.2018.03.003
- Zhan, Z. L., Deng, A. P., Kang, L. P., Tang, J. F., Nan, T. G., Chen, T., et al. (2018). Chemical Profiling in *Moutan Cortex* after Sulfuring and Desulfuring Processes Reveals Further Insights into the Quality Control of TCMS by Nontargeted Metabolomic Analysis. *J. Pharm. Biomed. Anal.* 156, 340–348. doi:10.1016/j.jpba.2018.04.045
- Zhang, X., Pi, Z., Zheng, Z., Liu, Z., and Song, F. (2018). Comprehensive Investigation of *In-Vivo* Ingredients and Action Mechanism of Iridoid Extract from *Gardeniae Fructus* by Liquid Chromatography Combined with Mass Spectrometry, Microdialysis Sampling and Network Pharmacology. *J. Chromatogr. B Analyt. Technol. Biomed. Life Sci.* 1076, 70–76. doi:10.1016/j.jchromb.2018.01.023
- Zhang, Y., Wei, Z., Liu, W., Wang, J., He, X., Huang, H., et al. (2017). Melatonin Protects against Arsenic Trioxide-Induced Liver Injury by the Upregulation of Nrf2 Expression through the Activation of PI3K/AKT Pathway. *Oncotarget* 8 (3), 3773–3780. doi:10.18632/oncotarget.13931
- Zheng, G., Liu, M., Chao, Y., Yang, Y., Zhang, D., Tao, Y., et al. (2020). Identification of Lipophilic Components in *Citri Reticulatae Pericarpium* Cultivars by Supercritical CO₂ Fluid Extraction with Ultra-high-performance Liquid Chromatography-Q Exactive Orbitrap Tandem Mass Spectrometry. *J. Sep. Sci.* 43 (17), 3421–3440. doi:10.1002/jssc.202000490
- Zheng, Y. Y., Zeng, X., Peng, W., Wu, Z., and Su, W. W. (2019). Characterisation and Classification of *Citri Reticulatae Pericarpium Varieties* Based on UHPLC-Q-TOF-MS/MS Combined with Multivariate Statistical Analyses. *Phytochem. Anal.* 30 (3), 278–291. doi:10.1002/pca.2812
- Zhou, J., Zhang, Y., Li, N., Zhao, D., Lu, Y., Wang, L., et al. (2020). A Systematic Metabolic Pathway Identification of Common *Gardenia* Fruit (*Gardeniae Fructus*) in Mouse Bile, Plasma, Urine and Feces by HPLC-Q-TOF-MS/MS. *J. Chromatogr. B Analyt. Technol. Biomed. Life Sci.* 1145, 122100. doi:10.1016/j.jchromb.2020.122100
- Zhou, J. L., Liu, W., Guo, Z. X., and Chen, B. L. (2013). Fingerprint Analysis of *Fritillaria Thunbergii* Using Rapid Resolution Liquid Chromatography Coupled with Electrospray Ionization Quadrupole Time-Of-Flight Tandem Mass Spectrometry. *Zhongguo Zhong Yao Za Zhi* 38 (17), 2832–2837. doi:10.4268/cjcm20131717

Conflict of Interest: The authors declare that the research was conducted in the absence of any commercial or financial relationships that could be construed as a potential conflict of interest.

Publisher's Note: All claims expressed in this article are solely those of the authors and do not necessarily represent those of their affiliated organizations, or those of the publisher, the editors and the reviewers. Any product that may be evaluated in this article, or claim that may be made by its manufacturer, is not guaranteed or endorsed by the publisher.

Copyright © 2022 Dong, Chen, Jiang, Zhu, Zheng, Zhang, Zhang, Chen, Sun, Pang, Yan, Liao and Fu. This is an open-access article distributed under the terms of the Creative Commons Attribution License (CC BY). The use, distribution or reproduction in other forums is permitted, provided the original author(s) and the copyright owner(s) are credited and that the original publication in this journal is cited, in accordance with accepted academic practice. No use, distribution or reproduction is permitted which does not comply with these terms.